

# DURABILITY OF CELLULOSE NANOMATERIALS UNDER INDUSTRY RELEVANT SHEAR STRESSES

Bradley P. Sutliff<sup>1,3</sup>, Arit Das<sup>3</sup>, Jeffrey Youngblood<sup>2</sup>, Michael J. Bortner<sup>1,3</sup>

<sup>1</sup>Macromolecules Innovation Institute, Virginia Tech, Blacksburg, VA, 24061, USA

<sup>2</sup>School of Materials Engineering, Purdue University, West Lafayette, IN 47907, USA

<sup>3</sup>Department of Chemical Engineering, Virginia Tech, Blacksburg, VA 24061

## Abstract

Composite materials rely heavily on the aspect ratios and orientations of their reinforcements. This makes it critically important to determine processing effects when investigating new discontinuous composite materials, such as those reinforced with cellulose nanomaterials (CNMs). The effects of high-shear flow on cellulose nanocrystals (CNCs) were studied to characterize potential impacts of industrial processing on these materials. A microcapillary rheometer was employed to study the rheological characteristics of aqueous CNC suspensions at concentrations ranging from 1.5 wt% to 12.1 wt%. Increased cellulose content in the suspensions produced increased viscosities. A Sisko model was successfully fit to the data which display high shear Newtonian plateaus. Shear rate sweeps at these concentrations failed to fully reduce to a master curve. Furthermore, repeated testing of the same sample volume at nearly  $800000\text{ s}^{-1}$  led to a permanent decrease in viscosity for all samples. Atomic Force Microscopy (AFM) probed CNC morphology to observe any changes in the CNC dimensions which may have contributed to this phenomenon. AFM results indicate significant decreases in both height and length of the CNCs after repeated testing at high shear rates, which would directly impact micromechanical models and anticipated reinforcing effects.

## Introduction

Automotive composites are tremendous tools to create strong and lightweight structures by combining various materials to obtain synergistic results. Carbon fiber composites have largely been the gold standard for racing materials, while glass fiber composites are more common to average consumers. One of the motivating forces for composite materials is the ability to drastically reduce weight while maintaining most or all of the mechanical strength and durability of a given part.[1] A discontinuous glass or carbon fiber composite can provide an equivalent bending stiffness to steel while reducing weight by up to 30 or 50%, respectively, and improving resistance to denting.[2] This can reduce fuel consumption for greener automobiles while preserving safety.

Furthermore, glass fibers have been used to enhance the structural integrity of both automotive parts and road surfaces.[3], [4]

Automotive manufacturers are also facing calls for less automotive waste and recyclability. [1] There currently exists a demand for renewable and biodegradable polymers, such that alternative materials which can be sustainably sourced and safely disposed of have gained significant interest. Cellulose, the material found in most plant cell walls, is a polymeric material that is naturally occurring and readily available. Nanocellulosics, in the form of cellulose nanocrystals (CNCs) and cellulose nanofibrils (CNFs), are extracted from the bulk cellulose. Mechanical and chemical manipulation of the raw cellulose yields nanoscale crystalline domains of bundled cellulose chains. The precise geometries and surface chemistries are dependent upon the source material and the extraction/production method[5]. Trees and plants supply the majority of CNCs, but tunicates, algae, and bacteria also generate these materials [5].

The biological origin of CNCs presents a renewable resource that should limit the impact of traditional plastics on the environment, while providing similar reinforcement capabilities to those of carbon and glass fibers. However, before CNCs become commonplace they must survive traditional processing environments. Industrial processes such as thermoforming, blow molding, and injection molding utilize shear rates from  $0.1\text{ s}^{-1}$  to  $10^6\text{ s}^{-1}$  [6]. Unfortunately, most rheological characterization of CNCs remains below  $100\text{ s}^{-1}$  [5]. The resulting stresses have the potential to align, degrade, or aggregate the CNCs. Alignment yields exploitable anisotropy, but degradation and alignment could negatively affect final product performance. However, if a certain level of degradation is expected, it can be accounted for during the design stage.

In this work, we investigate the effect of industrially relevant shear rates and subsequent shear stresses on aqueous CNC suspensions at concentrations from 1.5 wt% to 12.1 wt%. While characterizing the magnitude of the shear stresses on the nanocrystals, we also observe the morphological impacts of these stresses on the materials with atomic force microscopy (AFM).

## Materials

Never-dried sulfuric acid hydrolyzed cellulose nanocrystals originated from the USDA Forest Service-Forest Products Laboratory, Madison, WI, USA (Batch 098) and were received at a concentration of 12.1 wt% in water. These were obtained from hardwood pulp, with no additional additives. Conductometric titration was used to characterize the as-received CNCs following procedures outlined by CSA Group (2014) and Foster et al. (2018). They were found to have a surface sulfate density of 344 mmol/kg of CNC. Further analysis with atomic force microscopy revealed CNC average lengths of 159 nm and heights of 2.8 nm.

## Experimental Methods

### Rheological Measurements

A Rheosense e-VROC Viscometer equipped with an m-VROC E05 chip and a ThermoCube 300 temperature controller was used to characterize the viscosities of the CNC suspensions. The E05 chip has a flow channel depth of 50  $\mu\text{m}$  and a channel width of 3000  $\mu\text{m}$ . Four pressure sensors are located at 2.025 mm, 4.525 mm, 8.325 mm, and 10.825 mm from the entrance of the channel and allow measurements without entrance and exit pressure effects. 3 wt% CNC suspensions were characterized at apparent shear rates between 10000  $\text{s}^{-1}$  and 800000  $\text{s}^{-1}$ . For each concentration, CNC suspension temperature was maintained at 25  $^{\circ}\text{C}$ . For concentrations of 1.5, 6.0, and 12.1 wt%, 10 mL of material was repeatedly measured at the maximum shear rate to observe any changes in viscosity after prolonged exposure to elevated shear stresses. To avoid artifacts of shear rate ramping, the plateau regions were isolated from each dataset and used to calculate the average viscosity. The maximum Reynolds number for our datasets was calculated to be 442, ensuring that our sample flow remained laminar during all tests. The Weissenberg-Rabinowitsch-Mooney correction, Eq. 1, was used to correct for non-Newtonian behavior and to calculate true strain rates and viscosities for all relevant characterizations [7], [8].

$$\dot{\gamma} = \frac{\dot{\gamma}_{app}}{3} \left( 2 + \frac{d \ln \dot{\gamma}_{app}}{d \ln \tau_{app}} \right) \quad \text{Eq. 1}$$

In this equation  $\dot{\gamma}$  is the true shear rate,  $\dot{\gamma}_{app}$  the apparent shear rate, and  $\tau_{app}$  is the apparent shear stress at the wall.

Additionally, wall slip effects were assumed to be negligible given that wall depletion is most common with large particles, low shear rates, and large shear rate gradients [9]. This work focuses on nanoscale particles, high shear rates, and short gap heights, leading to the assumption that wall slip would not have a significant impact on the data.

### Atomic Force Microscopy

AFM was used to analyze CNCs after repeated shear measurements with an Asylum Research MFP-3D-Bio atomic force microscope. Height images were recorded in tapping mode (1 Hz, 512 scans, and 512 scans/line). The AFM was equipped with Olympus AC200TS R3 tips with a radius of 7 nm and a nominal spring constant 9 N/m. Uniform, dilute suspensions of CNCs were spin-coated onto poly-lysine-coated mica disks following Reid and Cranston's methods [5]. Mica discs were prepared as described in Section 5.2.4 of the Canadian Standard, Cellulosic Nanomaterials Test Methods for Characterization (CSA Z5100-14) (CSA Group, 2014). Gwyddion software was implemented to flatten the images and extract line profiles of isolated CNCs along their major axis. The average height along this length, was used to calculate the aspect ratio for each crystal. A minimum of 100 CNCs were characterized and their dimensions were averaged.

### Conductometric Titration

Conductometric titration was performed with established methods [5]. In brief, NaOH is added to CNC suspensions to determine the point of neutralization of the sulfate half ester groups. This neutralization point can then be used to calculate the mmol of sulfate half ester groups per kg of CNC,  $C_S$ , using Eq. 2, where  $V_{\text{NaOH}}$  is the volume in mL of NaOH needed to neutralize,  $C_{\text{NaOH}}$  is the mMolar concentration of the NaOH, and  $m_{\text{CNC}}$  is the mass of CNCs used in the test.

$$C_S = \frac{V_{\text{NaOH}} * C_{\text{NaOH}}}{m_{\text{CNC}}} \quad \text{Eq. 2}$$

## Results and Discussion

Steady shear rate measurements ranging from 10000  $\text{s}^{-1}$  to 800000  $\text{s}^{-1}$  at concentrations of 1.5, 3.0, 6.0, and 12.1 wt% CNC reveal the shear thinning behavior of the aqueous suspensions, followed by the onset of a high shear Newtonian plateau. The Sisko model, shown in Eq. 3, adds a correction to the power-law to account for this plateau with the addition of  $\eta_{\infty}$ , the high shear plateau viscosity [10], [11].

$$\eta = \eta_{\infty} + K \dot{\gamma}^{n-1} \quad \text{Eq. 3}$$

Data in Figure 1 highlight the concentration dependent viscosities along with the Sisko fits for each concentration ( $R^2 > 0.98$ ). Below  $10^5 \text{ s}^{-1}$ , shear thinning is the dominant behavior. However, at shear rates above  $10^5 \text{ s}^{-1}$  a Newtonian plateau is observed, most notably in the 1.5 and 3.0 wt% suspensions. Such phenomena are commonly associated with the orientation and alignment of the elongated particles along the direction of flow [12]. If higher shear rates produce a higher degree of alignment, at a critical shear rate a maximum number of nanocrystals may become aligned such that viscosity can no longer be lowered via orientation of the particles. Above this critical

rate, the carrier fluid would dominate the behavior of the suspension. At higher concentrations, there are more particles to align and therefore a higher shear rate is required to align a critical percentage of the nanocrystals.

Approximately 10 ml of the 12.1, 6.0, and 1.5 wt% suspensions were recycled at the maximum possible shear rate up to 15 times. This number of repeats sufficiently verified viscosity changes from exposure to

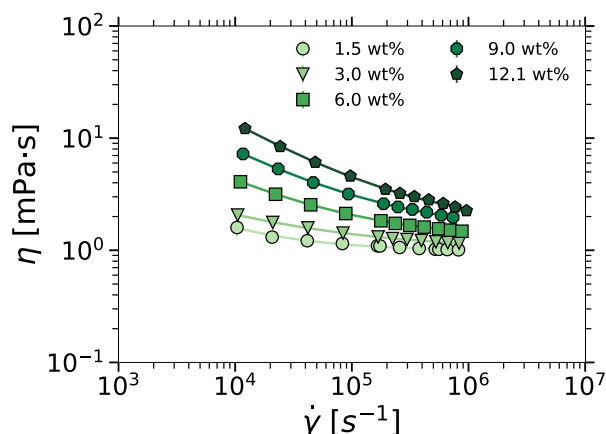


Figure 1: Viscosity measurements of aqueous CNC suspension in concentrations ranging from 1.5 to 12.1 wt%, and over a shear rate range of  $10^4 \text{ s}^{-1}$  to  $8 \times 10^5 \text{ s}^{-1}$  at  $25 \text{ }^\circ\text{C}$ . Sisko model fits are shown as solid lines.

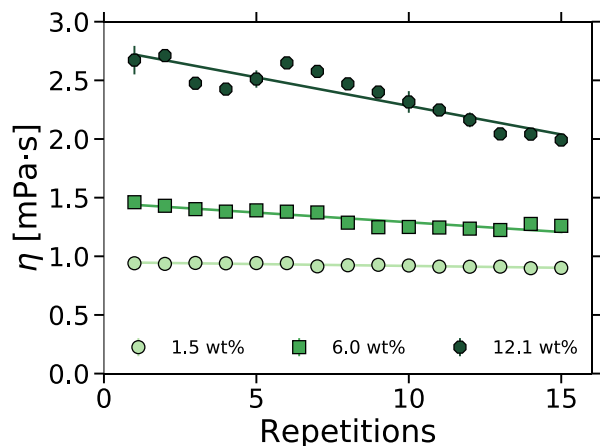


Figure 2: Viscosity of various CNC wt% suspensions after repeated exposure to shear rates approaching  $800000 \text{ s}^{-1}$ . Solid lines represent linear fits to the respective datasets.

high shear stresses. The change in the average viscosity of the suspension after each measurement is reported in Figure 2. A significant reduction of viscosity is observed in the 12.1 wt% sample. The 6.0 wt% sample displays a slower decrease in viscosity, while the 1.5 wt% sample remains at an almost constant viscosity. To rule out the possibility of insufficient relaxation times, measurements were stopped after 7-9 runs and allowed to relax up to two

weeks before resuming. As observed in Figure 2, the original viscosity is not recovered.

The decrease in viscosity leads to questions about the possibility of damage to the particles at high shear. Therefore, AFM was employed to characterize the 12.1 wt% CNC suspensions and observe any morphological changes in the CNCs. Representative images of the highly diluted 12.1 wt% suspensions can be seen in Figure 3.

Analysis of 100+ individual nanocrystals reveals

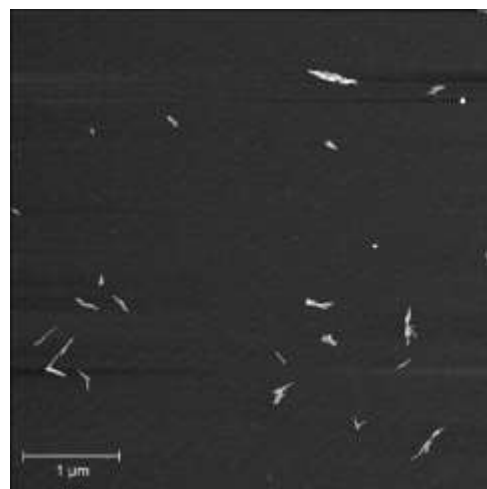


Figure 3: Representative images of 00-cycle CNCs obtained from AFM. Isolated CNCs are characterized in Gwyddion for length and height profile to identify any changes in the dimensions of the CNCs after 15 cycles.

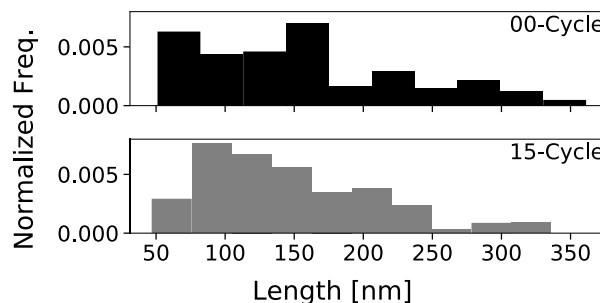


Figure 4: Histograms of the measured lengths for the CNCs before (top) and after (bottom) 15-cycles of high shear rate testing.

that 00-cycle specimens had an average height of  $2.8 \pm 1.0 \text{ nm}$ , while the 15-cycle specimens have an average height of  $2.5 \pm 1.0 \text{ nm}$ . Furthermore, the average length of the 00-cycle crystals was  $159 \pm 75 \text{ nm}$  and the 15-cycle were  $146 \pm 64 \text{ nm}$  long. Additionally, the histograms of all CNC length measurements are displayed in Figure 4, illustrating the decrease of high-length crystals after only 15 high-shear rate repetitions. This decrease in both average sizes and size distributions could lead to the decrease in viscosity [12]. Further, the population of short CNCs appears to have decreased, which could be due to total disintegration of the CNCs or measurement error

arising from an inability to distinguish such short CNCs from artifacts on the sample surface.

Conductometric titration was also performed on both samples. These titrations demonstrated that while CNC size may have been affected, surface charge density was not significantly different according to the 5% error associated with the measurement technique [13]. Since the surface charges are not affected by the shear stresses, we can attribute the majority of the viscosity changes to the change in physical dimensions of the CNCs.

It should be noted that the lower concentrations have fewer CNCs present, and lower total stress at the same shear rate compared to higher concentrations: 744 Pa, 1155 Pa, and 2114 Pa respectively for the 1.5, 6.0, and 12.1 wt% samples during the first set of measurements, e.g. 00-cycle. Therefore, reduced concentration and the corresponding reduced stresses would be expected to have a reduced impact on the CNC size change and are expected to display a smaller scale change in viscosity, as observed in Figure 2.

## Conclusions

As expected, increased concentrations result in higher viscosities of the CNC suspensions. Lower concentrations exhibit high shear rate Newtonian plateaus that indicate a critical shear rate where the CNCs are aligned to such a high extent that no more alignment driven shear-thinning is possible. Above this rate, orientation of the CNCs is presumably prevalent enough that increased rates do not yield noticeable increases in orientation. This leads to limited decreases in viscosity as shear rates increase.

Further, repeated testing of the CNCs at the highest instrument-obtainable shear rate has demonstrated that shear stresses can affect the morphology of the CNCs. Increased exposure to the high shear rates resulted in decreased viscosities of the suspensions and decreased height and length of the individual CNCs.

These two observations must be kept in mind as these materials move into commercial use. If CNCs are to be used with current polymer processing techniques and their associated stresses, they may be expected to change morphology as they are processed. This may not hinder their adoption as bio-friendly additives, but such effects will certainly need to be accounted for before processing parameters can be finalized.

## References

[1] A. K. Bledzki, O. Faruk, and V. E. Sperber, "Cars from Bio-Fibres," *Macromol. Mater. Eng.*, vol. 291, no. 5, pp. 449–457, May 2006.

[2] L. T. Harper, "Discontinuous Carbon Fibre Composites for Automotive Applications," PhD, the University of Nottingham, 2006.

[3] M. R. Mansor, S. M. Sapuan, E. S. Zainudin, A. A. Nuraini, and A. Hambali, "Hybrid natural and glass fibers reinforced polymer composites material selection using Analytical Hierarchy Process for automotive brake lever design," *Mater. Des.*, vol. 51, pp. 484–492, Oct. 2013.

[4] A. Mahrez, M. R. Karim, and H. Y. bt Katman, "FATIGUE AND DEFORMATION PROPERTIES OF GLASS FIBER REINFORCED BITUMINOUS MIXES," *Journal of the Eastern Asia Society for Transportation Studies*, vol. 6, pp. 997–1007, 2005.

[5] E. J. Foster *et al.*, "Current characterization methods for cellulose nanomaterials," *Chem. Soc. Rev.*, vol. 47, no. 8, pp. 2609–2679, Apr. 2018.

[6] A. Franck, "Understanding Rheology of Thermoplastic Polymers," TA Instruments, AAN013, 2004.

[7] C. W. Macosko, *Rheology: Principles, Measurements, and Applications*. New York: Wiley-VCH, Inc, 1994.

[8] R. A. Mendelson, F. L. Finger, and E. B. Bagley, "Die swell and recoverable shear strain in polyethylene extrusion," in *Journal of Polymer Science: Polymer Symposia*, 1971, vol. 35, pp. 177–188.

[9] H. A. Barnes, "A review of the slip (wall depletion) of polymer solutions, emulsions and particle suspensions in viscometers: its cause, character, and cure," *J. Non-Newtonian Fluid Mech.*, vol. 56, no. 3, pp. 221–251, Mar. 1995.

[10] S. Shareghi and D. Toghraie, "Numerical Simulation of Blood Flow in Healthy Arteries by us of the Sisko Model," *CTS*, vol. 8, no. 4, 2016.

[11] N. Ali, A. Zaman, and M. Sajid, "Unsteady blood flow through a tapered stenotic artery using Sisko model," *Comput. Fluids*, vol. 101, pp. 42–49, Sep. 2014.

[12] N. Willenbacher and K. Georgieva, "Rheology of Disperse Systems," in *Product Design and Engineering*, vol. 52, U. Bröckel, W. Meier, and G. Wagner, Eds. Weinheim, Germany: Wiley-VCH Verlag GmbH & Co. KGaA, 2013, pp. 7–49.

[13] L. J. Johnston *et al.*, "Determination of sulfur and sulfate half-ester content in cellulose nanocrystals: an interlaboratory comparison," *Metrologia*, vol. 55, no. 6, p. 872, Nov. 2018.